Colloid Polym Sci 279:546–553 (2001)

ORIGINAL CONTRIBUTION

X. Zhu
D. Yan

Influence of the order of polymer melt on the crystallization behavior: II. Crystallization kinetics of isotactic polypropylene

Received: 16 June 2000
Accepted: 16 October 2000

X. Zhu · D. Yan (✉)
College of Chemistry
and Chemical Technology
Shanghai Jiao Tong University
800 Dongchuan Road
Shanghai 200240
People's Republic of China
e-mail: dyyan@mail.sjtu.edu.cn
Tel.: +86-21-5474-2665
Fax: +86-21-5474-1297

Abstract The crystallization behavior of isotactic polypropylene (iPP) melts with a high order has been carefully examined by differential scanning calorimetry (DSC) and polarized light microscopy (PLM). The experimental results show that the helically ordered iPP melt crystallizes by heterogeneous nucleation with two-dimensional diffusion controlled growth and the Avrami exponent is about 2. The data available both from our DSC and PLM experiments and from the literature indicate that the order of a polymer melt can speed up the crystallization process. When some unmelted materials exist in the ordered melt, the crystallization will become more rapid.

Key words Isotactic polypropylene · Polymer melt · Crystallization kinetics · Avrami analysis

Introduction

Considerable attention has been focused on the crystallization kinetics of isotactic polypropylene (iPP) because of its importance in both mechanism studies and the processing of polymers [1–30]. In 1959, Marker [1], Griffith [2], and Falkai et al. [3] adopted the dilatometry and optical microscopy methods, respectively, to examine the crystallization behavior of iPP at different temperatures. They found that the crystallization follows the kinetics of a nucleation-controlled process according to the Avrami equation and that the corresponding Avrami exponent is 3. Since then, many other methods such as light depolarization microscopy (LDM) [4, 10], infrared microscopy (IR) [13], differential scanning calorimetry (DSC) [9–10, 14–17], and differential thermal analysis (DTA) [6] have also used in this field of research. Generally, the crystallization of isotactic polypropylene is heterogeneous, athermal nucleation followed by a three-dimensional spheralitic crystal growth and the Avrami exponent is equal to 3.

Griffith et al. [2] found that an iPP sample with a lower molecular weight has a more rapid crystallization. Subsequently, Parrini and Corrieri [5] observed that, compared with a polydisperse sample, the narrow distribution sample has a lower crystallization rate. Based on the observations of optical microscopy and X-ray diffraction, Hoshino et al. [8] proposed that the crystallization of iPP consists of two stages: primary crystallization and secondary crystallization. Both primary and secondary crystallization can be well described by the Avrami equation, while the Avrami exponent of the former is larger than that of the latter. However, Martuscelli and Avella [15–17] pointed out that the secondary crystallization occurs only in a lower degree of stereoregularity, which suggests that the secondary crystallization results from the presence of some configurational irregularity in the iPP chains. These authors [15–17] have systematically investigated the influence of the degree of stereoregularity on the overall rate of crystallization, and concluded that at constant crystallization temperature the overall rate constant of crystallization decreases with the increase of configurational chain defects. Moreover, the recrystallization kinetics of partially melting iPP reveal that the crystallization process can be accelerated by the existence of unmelted materials [18, 30]. Recently, many studies have been focused upon the relationship of nucleating agents or additives with crystallization behavior [14, 19, 21–26]. It is found that the addition of nucleating agents or

additives will increase the nucleation density and crystallization rate.

Even though the crystallization kinetics of iPP have been extensively studied during the past decades of years, no attention has been paid to the relation between the order of the polymer melt and the crystallization behavior. The main aim of the present research is to study the crystallization kinetics of a helically ordered melt, in order to analyze the influence of the order of the polymer melt on the kinetic parameters controlling the crystallization process of the iPP sample.

Materials and methods

The isotactic polypropylene (iPP) used in this study was kindly provided by Shanghai Jinshan Petrochemical Corp. (Shanghai, P. R. China). The material is highly isotactic, being approximately 94.5% insoluble in *n*-heptane and has a melt flow index of 3.0 g/10 min. To erase the previous thermomechanical history, a film of melted polymer about 300 μm thick was pressed between two glass slides at 210 °C for 10 min in a hot stage, and then rapidly transferred to another hot stage that was set at 130 °C. After having crystallized for half an hour, the sample was quenched to 0 °C.

The crystallization kinetics study was carried out on a Perkin-Elmer Pyris-1 Series differential scanning calorimeter under a flowing nitrogen atmosphere. The iPP sample, crystallized at 130 °C for half an hour, was heated to 169 °C or 210 °C, respectively, and then quickly cooled to different crystallization temperatures (T_c) for isothermal crystallization or cooled to 20 °C at different cooling rates. The DSC was calibrated using In and Zn as standards. For all experiments, the sample weights were approximately 5 mg and the heating rate was 10 °C/min.

The morphological studies were performed on an optical polarized Leika microscope, with a Leika hot-stage thermal control. The iPP sample, crystallized at 130 °C for half an hour, was sandwiched between two microscope cover glasses, heated to 169 °C or 210 °C, respectively, and then rapidly cooled to 131 °C for isothermal crystallization.

Results

Our recent findings [30–33] have pointed out that when the iPP sample, isothermally crystallized at 130 °C for half an hour, is heated to 169 °C, the polymer crystalline material is melted while the helical structure of the individual macromolecular chain can be well retained. The multiple melting behaviors observed in the first part of this series further confirm the existence of a helically ordered melt [34]. Given an appropriate supercooling degree, these helically ordered iPP melts would crystallize. Fig. 1 shows the heat flow change for the isothermal crystallization at various temperatures. It can be seen that the iPP melt crystallizes very quickly and there is no induction period for every curve. When $T_c \leq 123$ °C, the crystallization proceeds so rapidly that a considerable amount of crystallinity is produced during the cooling process. Therefore, the isothermal analysis is performed at every 2 °C in the temperature interval 123–131 °C.

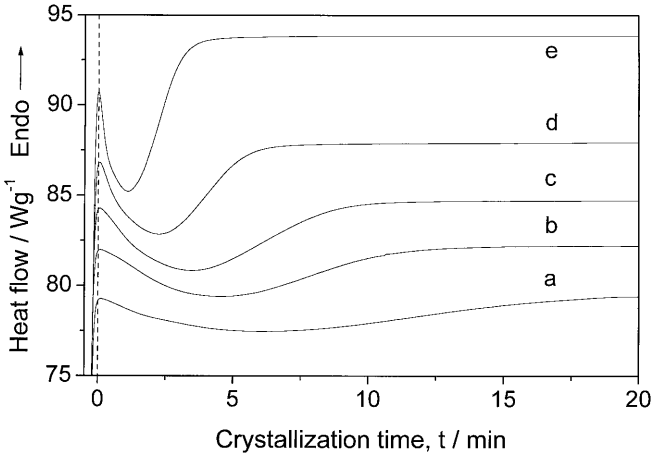

Fig. 1 Time dependence of the heat flow for the isothermal crystallization of a helically ordered iPP melt at: (a) 131 °C; (b) 129 °C; (c) 127 °C; (d) 125 °C; (e) 123 °C

The relative amount of crystallinity has been plotted as a function of time for five different crystallization temperatures (see Fig. 2). The development of the relative crystallinity during the isothermal process can be analyzed by the Avrami equation (Eq. 1) [35–36]:

$$X_t = 1 - \exp(-kt^n) \tag{1a}$$

$$\text{or } \log[-\ln(1 - X_t)] = \log k + n \log t \tag{1b}$$

where X_t is the relative volume-fraction crystallinity at time t, n is a constant whose value depends on the mechanism of nucleation and on the form of crystal growth, and k is a constant containing the nucleation and growth parameters. The double logarithmic plot of $\log[-\ln(1 - X_t)]$ versus logt is shown in Fig. 3 and each

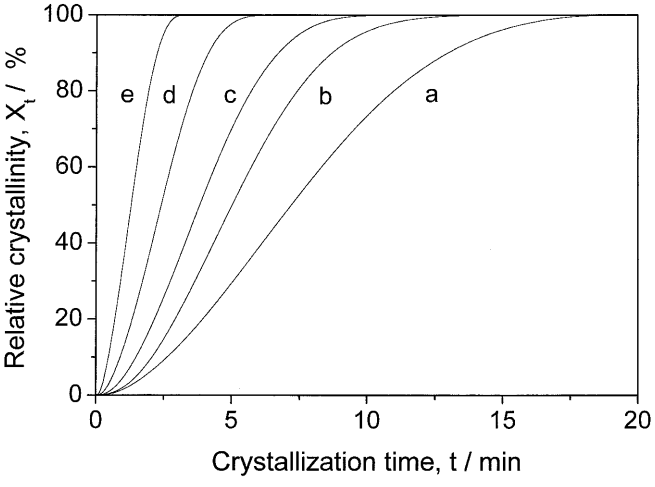

Fig. 2 Relative crystallinity versus time during isothermal crystallization of a helically ordered iPP melt at different temperatures: (a) 131 °C; (b) 129 °C; (c) 127 °C; (d) 125 °C; (e) 123 °C

curve presents a single straight line. The values of n and k are determined from the slope and intercept of each straight line, and the results are summarized in Table 1. Interestingly, the Avrami parameter n is about 2. Generally, $n = 3$ is found for crystallization from an unperturbed equilibrium iPP melt. The lower Avrami exponent ($n = 2$) means that the crystallization mechanism of the helically ordered iPP melt is distinct from that of the unperturbed equilibrium melt.

The necessary time for maximum crystallization t_{max} can be obtained directly from the heat-flow curves or be calculated from the Eq. 2:

$$t_{max} = [(n-1)/nk]^{1/n} \quad (2)$$

The term t_{max} corresponds to the point of the heat-flow curve where $dQ(t)/dt = 0$ and Q(t) is the heat-flow rate. Both the directly observed and calculated values are listed in Table 1. The agreement in t_{max} values suggests that the Avrami analysis works well in describing the isothermal crystallization kinetics of a helically ordered iPP melt. In addition, t_c and $t_{1/2}$ can also be used to describe the rate of crystallization. Crystallization continues until the time t_c at which no further heat flow is observed. The crystallization half-time $t_{1/2}$ is defined as the time at which the extent of crystallization is 50% completed. It can be derived directly from Fig. 2 or determined from the measured kinetics parameter (Eq. 3), that is:

$$t_{1/2} = (\ln 2/k)^{1/n} \quad (3)$$

Usually, the rate of crystallization G is described as the reciprocal of $t_{1/2}$; i.e., $G = \tau_{1/2} = t_{1/2}^{-1}$. The values of t_c, $t_{1/2}$ and G are also listed in Table 1. With increasing temperature, t_{max}, t_c and $t_{1/2}$ increase whereas the rate of crystallization G decreases.

Table 1 shows that the rate constant k increases with decreasing crystallization temperature. If the crystallization process is assumed to be thermally activated, the crystallization activation energy can be obtained by the Arrhenius equation (Eq. 4) [37]:

$$k^{1/n} = k_0 \exp(-\Delta E/RT_c) \quad (4a)$$

$$\text{or } (1/n)\ln k = \ln k_0 - (\Delta E/RT_c) \quad (4b)$$

where k_o is a temperature independent preexponential factor, R is the gas constant, T_c is the absolute temperature, and ΔE is the crystallization activation energy. Figure 4 shows the plot of (1/n)ln k vs. $1/RT_c$. From the slope of the straight line, the crystallization activation energy is found to be 312 kJ/mol.

In order to validate the isothermal analysis, the non-isothermal crystallization of a helically ordered iPP melt has been performed as described below. Figure 5 shows the cooling crystallization curve of a helically ordered iPP melt at various cooling rates. With increasing cooling rate, the crystallization peak shifts to the lower temperature. Considering the fact that the free spherulitic growth approximation is valid at a low degree of conversion [37], the initial stage of non-isothermal crystallization can be described by the Avrami equation [35–36]. The double logarithmic plot of $\log[-\ln(1 - X_t)]$ versus logt for non-isothermal crystallization is shown in Fig. 6. Each curve has an initial linear section and the

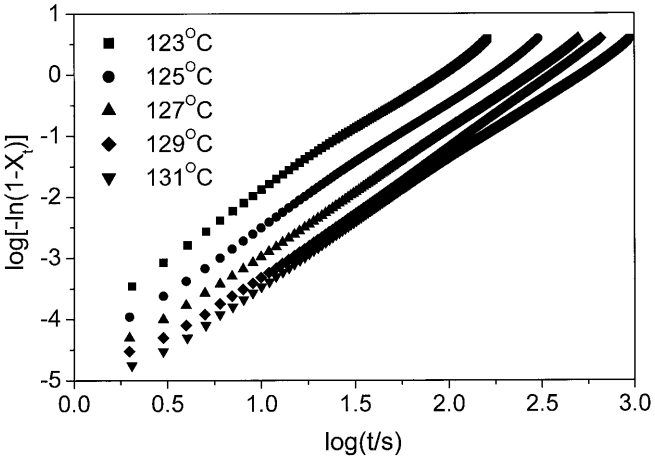

Fig. 3 Plots of $\log[-\ln(1 - X_t)]$ vs. logt for the isothermal crystallization of a helically ordered iPP melt

Table 1 Parameters from the Avrami analysis of isothermal crystallization

T_c [°C]	131	129	127	125	123
n	2.0	2.1	2.1	2.0	2.1
k [s^{-n}]	3.98×10^{-6}	4.07×10^{-6}	7.59×10^{-6}	3.39×10^{-5}	9.77×10^{-5}
t_{max}[a] [min]	6.07	4.57	3.47	2.29	1.10
t_{max}[b] [min]	5.91	4.52	3.36	2.02	1.01
t_c [min]	19.41	16.71	12.68	8.80	5.23
$t_{1/2}$[a] [min]	7.14	5.01	3.81	2.39	1.28
$t_{1/2}$[b] [min]	6.95	5.16	3.84	2.38	1.14
G [min^{-1}]	0.14	0.20	0.26	0.42	0.78

[a] Determined from the Fig. 2
[b] Calculated from the Avrami parameters

Avrami parameters n and k can be determined from the slopes and intercepts of the linear portion. Table 2 reveals that the Avrami exponent n ranges from 2.0 to 2.2 with different cooling rates, agreeing with the result of the isothermal analysis very well. The rate constant k decreases with decreasing cooling rate. Based on the various k values at different cooling rates, the crystallization activation energy can be obtained by the Arrhenius equation [37]. Figure 7 is the plot of (1/n)lnk vs. $1/RT_c$ for the non-isothermal crystallization. From the slope of the straight line, the crystallization activation energy is found to be 347 kJ/mol. On the other hand, the Kissinger method (Eq. 5)can also be used to determine the activation energy of non-isothermal crystallization [38]:

$$d[\ln(\Phi/T_p^2)/d(1/T_p)] = -\Delta E/R \quad (5)$$

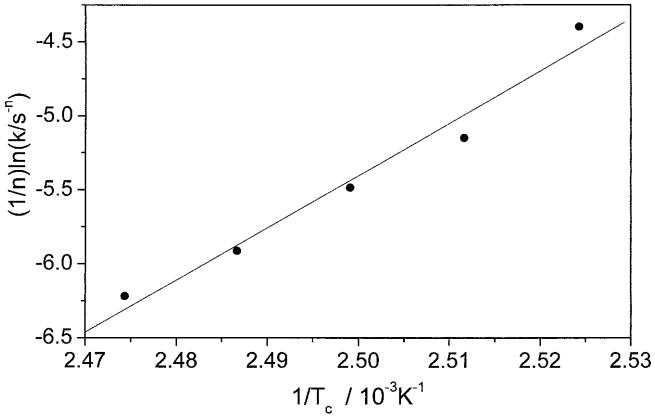

Fig. 4 Plot of (1/n)lnk versus $1/T_c$ for the Avrami analysis of isothermal crystallization of a helically ordered iPP melt

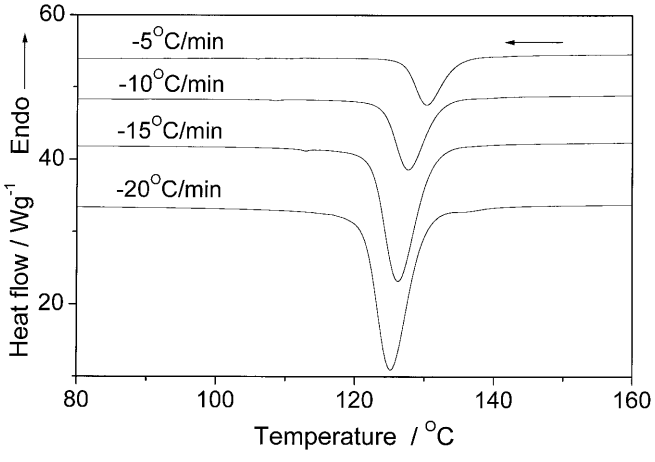

Fig. 5 Heat flow versus temperature during non-isothermal crystallization of a helically ordered iPP melt at different cooling rates

where Φ is the cooling rate, T_p is the cooling peak temperature and R is the gas constant. Figure 8 is the graph of $\ln(\Phi/T_p^2)$ against $1/T_p$. According to the slope of the curve, the activation energy is determined as 352 kJ/mol. The agreement in ΔE values determined by Avrami and Kissinger methods demonstrates that the Avrami analysis works well in describing the initial stage of non-isothermal crystallization of a helically ordered iPP melt.

If the iPP sample, crystallized at 130 °C for half an hour, was heated to 210 °C and then cooled to 131 °C for isothermal crystallization, the crystallization behavior would be altered. Table 3 shows the influence of fusion temperature on the subsequent crystallization. It can be found that, with increasing fusion temperature, the Avrami exponent changes from 2 to 3 and the crystallization becomes slower. Figure 9 shows the micrographs of an iPP sample that was heated to different fusion temperatures (169 °C and 210 °C, respectively) and then cooled to crystallize at 131 °C for an hour. It is apparent that the number of spherullites in Fig. 9a is more than the counterpart in Fig. 9b. So the lower fusion temperature corresponds to a faster primary nucleation rate.

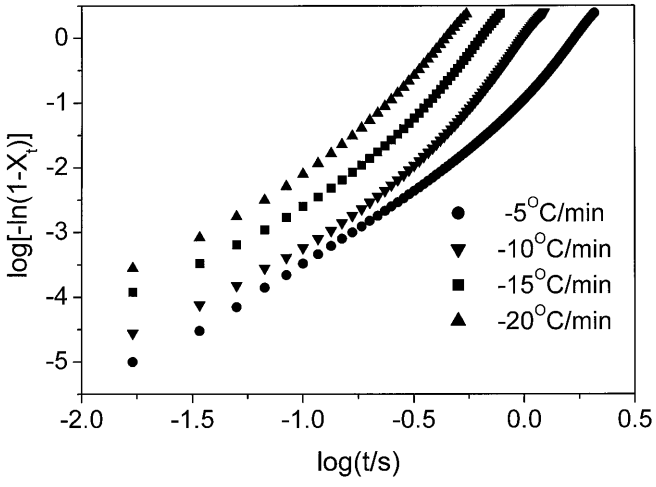

Fig. 6 Plots of $\log[-\ln(1 - X_t)]$ vs. logt for non-isothermal crystallization of a helically ordered iPP melt

Table 2 Parameters from the Avrami analysis of non-isothermal crystallization

Φ [°C min^{-1}]	T_p [°C]	n	k [s^{-n}]	$\Delta E^{[a]}$ [kJ mol^{-1}]	$\Delta E^{[b]}$ [kJ mol^{-1}]
5	130.5	2.1	1.36×10^{-5}		
10	127.8	2.2	3.19×10^{-5}		
15	126.3	2.0	8.01×10^{-5}	347	352
20	125.1	2.0	2.48×10^{-4}		

[a] Determined by the Avrami equation
[b] Determined by the Kissinger equation

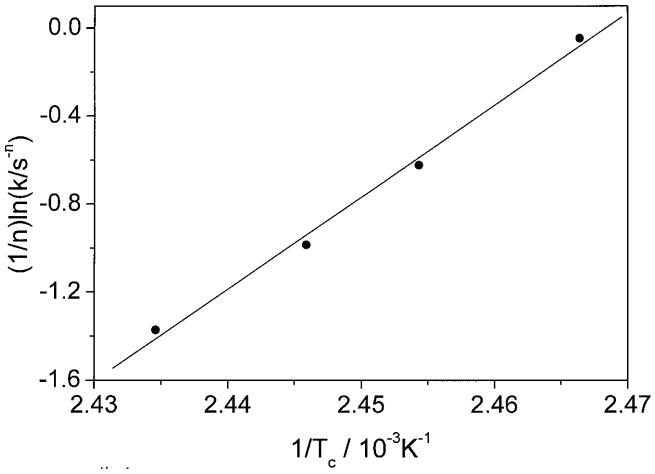

Fig. 7 Plot of (1/n)lnk versus $1/T_c$ for the Avrami analysis of non-isothermal crystallization of a helically ordered iPP melt

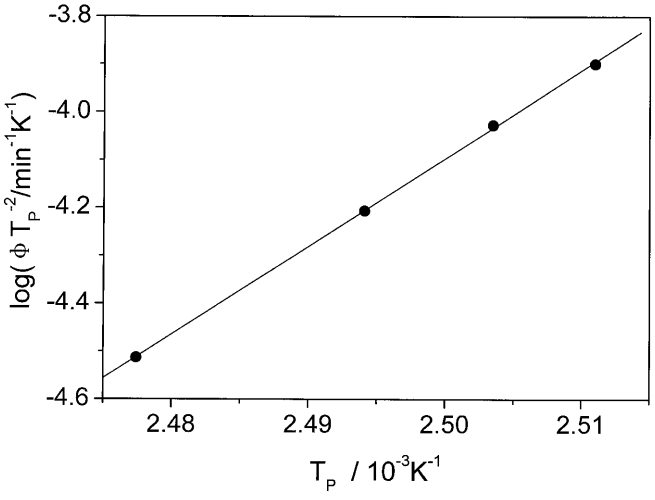

Fig. 8 Kissinger graph for evaluating the non-isothermal crystallization activation energy of a helically ordered iPP melt

Discussion

Both the isothermal and non-isothermal analysis in this study show that the Avrami exponent is about 2, which means that the helically ordered iPP melt exeriences heterogeneous, athermal nucleation followed by a two-dimensional diffusion controlled growth. Such a low Avrami value has ever been reported in the past: In 1984, Carfagna et al. [18] adopted the dilatometric technique to study the recrystallization kinetics of iPP; using the calorimetric method and we have examined the crystallization behavior of partially melting iPP [30]. In both cases, the fusion temperatures are lower and the corresponding Avrami exponents for low crystallinity are approximately 2. Table 4 lists the available experimental sources from the literature based on various methods. It can be seen that, on raising the fusion temperature, the Avrami exponent becomes larger. It is usually assumed that some unmelted crystals still exist at a lower fusion temperature. The existing crystals can serve as nuclei so that the molecular chains in the melt can crystallize from the edge or surface of crystals. Accordingly, the Avrami exponent is small. As the fusion temperature is elevated, the conditions for nucleation become more critical and less nucleation

Table 3 The effect of fusion temperature on the subsequent isothermal crystallization

T_f [°C]	T_c [°C]	n	k [s^{-n}]	t_{max} [min]	$t_{1/2}$ [min]	G [min^{-1}]
169	131	2	3.98×10^{-6}	5.91	6.95	0.144
210	131	3	9.31×10^{-9}	6.92	7.36	0.136

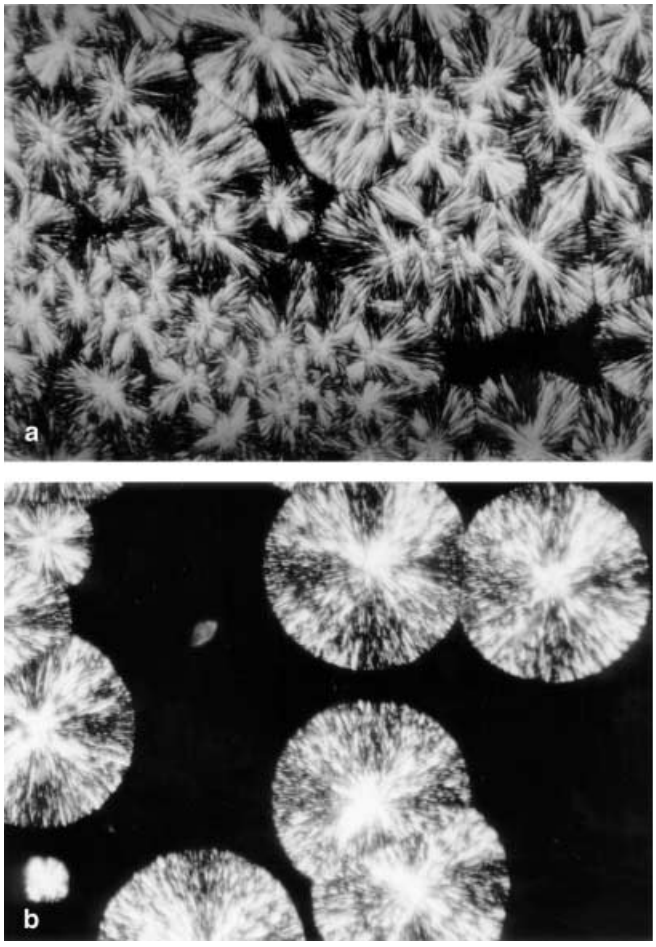

Fig. 9 Micrographs for an iPP sample (400×) which is crystallized at 130 °C for half an hour, heated to different fusion temperature: (a) 169 °C; (b) 210 °C, and then isothermally crystallized at 131 °C for an hour

Table 4 Summary of isothermal crystallization data for isotactic polypropylene

Reference	Method[a]	T_c [°C]	$t_{1/2}$ [min]	k [s^{-n}]	n	T_f [°C]
Marker et al. (1959) [1]	dilat. and POM	123		2.69×10^{-8}	3	220
		125		7.59×10^{-9}		
		127		1.42×10^{-9}		
		132		9.33×10^{-11}		
Griffith and Ranby (1959) [2]	dilat. and POM	133	10.6	2.69×10^{-9}	3	190
Falkai and Stuart (1959) [3]	dilat. and POM	122		2.67×10^{-7}	3	180
		125		5.23×10^{-8}		
		127.5		6.76×10^{-9}		
		130		1.31×10^{-9}		
		132.5		2.49×10^{-10}		
Magill (1962) [4]	LDM	121.5	1.67	8.0×10^{-6}	3	270
		124	3.95	8.15×10^{-8}		
		130.5	12.50	2.15×10^{-9}		
Parrini and Corrieri (1963) [5]	dilat.	130	7	4.68×10^{-9}	3	190
		130	12	1.53×10^{-9}	3.1	210
Chiu (1964) [6]	DTA	123	1.4			260
Gordon and Hillier (1965) [7]	dilat.(unseeded)	134		5.16×10^{-9}	2.5	
	(seeded)	143.5		1.85×10^{-11}	3	
Hoshino et al. (1965) [8]	dilat.	120	17.78		3.9	0
		124	50.12			
		127	112.2			
		130	141.3			
Godovsky et al. (1974) [9]	dilat.	130.2	13	8.61×10^{-10}	3.1	190
Pratt and Hobbs (1976) [10]	DSC	120	1.2	1.0×10^{-5}	2.9	210
		125	2.51	1.23×10^{-7}	2.9	
		130	12.02	1.58×10^{-9}	2.7	
	LDM	120	1	6.31×10^{-6}	3.0	210
		123	1.58	6.31×10^{-7}	2.9	
		125	1.82	2.51×10^{-7}	2.9	
		127	3.98	3.98×10^{-8}	2.9	
		130		3.16×10^{-9}	3.0	
Ishizuka and Koyama (1977) [12]	DSC				3.1	250
Wlochowicz and Eder (1981) [13]	IR	122	4.03	2.37×10^{-8}	3.12	185
		125	6.78	8.39×10^{-9}	3.03	
		127	9.35	4.83×10^{-9}	2.97	
		130	16.28	5.09×10^{-10}	3.05	
		132	25.48	1.56×10^{-10}	3.03	
Rybnikar (1982) [14]	LDM	137	9		3.0	220
Martuscelli et al. (1983) [15]	DSC	122.4	3.83	5.89×10^{-8}	3.4	215
		124.4	6.33	1.29×10^{-8}	3.0	
		126.4	9.17	4.27×10^{-9}	3.0	
		128.4	16.83	6.61×10^{-10}	2.7	
		129.4	21.67	3.09×10^{-10}	2.7	
Avella et al. (1983) [16]	DSC	123	1.77	1.3×10^{-5}	2.5	190
		125	2.73	3.7×10^{-6}	2.5	
		127	3.9	1.6×10^{-6}	2.5	
		129	6.87	2.6×10^{-7}	2.5	
		131	11.12	3.9×10^{-7}	2.5	
Carfagna et al. (1984) [18]	dilat.	161		4.52×10^{-5}	1.6	161
		163		1.88×10^{-5}	1.6	163
		165		1.40×10^{-5}	1.6	165
		167		4.52×10^{-7}	1.6	167
Kowalewski et al. (1986) [19]	DSC	130		2.84×10^{-9}	2.71	230
Tai et al. (1991) [23]	DSC	122	3.478	7.35×10^{-8}	3	220
		124	4.834	2.83×10^{-8}		
		126	8.656	5.77×10^{-9}		
		128	12.41	1.69×10^{-9}		
		130	19.89	7.12×10^{-10}		
		132	26.74	1.60×10^{-10}		
Kim et al. (1993) [26]	DSC	128.3		6.82×10^{-7}	2.45	0
		126		8.39×10^{-8}	2.74	
		127.9		5.56×10^{-8}	2.42	
		129.7		7.52×10^{-9}	2.59	
		132		2.09×10^{-9}	2.56	
Hieber (1995) [27]	simulation				3	

[a] Abbreviations: dilat = dilatometry, POM = polarized optical microscopy, LDM = light depolarizing microscopy, DTA = differential thermal analysis, DSC = differential scanning calorimetry, IR = infrared spectroscopy

sites become available, leading to the increase of the Avrami exponent. However, many researchers [14, 19, 21, 23, 26] have observed that the addition of nucleating agents or additives does not diminish the Avrami exponent. Additionally, it has been well established that the Avrami exponent of partially melting polymers, including PE [39], PET [40], PEEK [41], and Nylon [42], is approximately 1. Hence, the crystallization behavior of a polymer melt should be related to the molecular structure of different polymers. Recently, we [30–33] have studied the melting process of a crystallized iPP sample. It was found that, although the inter-stem interaction of lamellae is destroyed after the melting of crystalline iPP, the intra-stem interaction is still maintained; thus, the melt is of a helically ordered structure. As soon as the temperature is higher than 170.5 °C, the macromolecules get enough energy from the surroundings to overcome the intra-stem interaction. As a result, the helically ordered structure of the individual molecular chains is reduced dramatically and the order of the polymer melt decreases greatly. It is possible that the difference in the order of the polymer melt will affect the subsequent crystallization behavior. When the fusion temperature is lower than 170.5 °C, the iPP melt is of a helically ordered structure, so the crystallization proceeds by two-dimensional diffusion controlled growth and the Avrami exponent is 2. If the temperature is higher than 170.5 °C, the helically ordered structure of the melt is destroyed and the order of the polymer melt is decreased greatly. Consequently, the crystal growth is three-dimensional and the Avrami exponent is 3 or 4, depending on the predetermined or sporadic nucleation (see Tables 3 and 4). As for PE, PET, PEEK, and Nylon, at a lower fusion temperature the conformation of molecules in the melt is planar zig-zag, thus the crystal growth is one-dimensional and the Avrami exponent is 1. With increasing temperature, the amount of the *gauche* conformation increases, therefore the order of the polymer melt decreases and the corresponding Avrami exponent becomes larger.

The rate constants k for various cases are also listed in Table 4, they range from 10^{-5} to 10^{-14}. Compared with the literature data at the same crystallization temperature, the k value of the helically ordered melt is much larger, which can be further confirmed by the data listed in Table 3. Fig. 9 also shows that the primary nucleation rate of a helically ordered melt is higher than that of an unperturbed equilibrium melt. All of these results demonstrate that the order of the polymer melt can speed up the crystallization process. The comparison of rate constants in the non-isothermal crystallization processes (see Table 5) shows that if some unmelted materials exist in the helically ordered melt, the rate constant will become much larger. Therefore, both the ordered structure of the polymer melt and the residual crystals can accelerate the crystallization process, which is in agreement with our recent observation on the crystallization behavior of a partially melting iPP sample [30].

Conclusions

The Avrami analysis of the crystallization kinetics of a helically ordered iPP melt has been carried out by means of differential scanning calorimetry (DSC) and polaried light microscopy (PLM). It is found that the iPP melt with a helically ordered structure crystallizes faster than the unperturbed equilibrium melt, and that the Avrami equation describes both the isothermal and non-isothermal crystallization very well. The Avrami exponent is about 2, which means that the crystallization of a helically ordered iPP melt involves heterogeneous nucleation with two-dimensional diffusion controlled growth. With increasing crystallization temperature in the isothermal crystallization process, t_{max}, t_c and $t_{1/2}$ increase whereas k and G decrease. On the other hand, with decreasing cooling rate in the non-isothermal crystallization, the crystallization becomes slower.

If the iPP sample is heated to a high temperature, the subsequent crystallization behavior is altered greatly. With increasing fusion temperature, the Avrami exponent changes from 2 to 3 and the crystallization process becomes slower.

In order to explain the aforementioned experimental results, a possible mechanism based on the order of the polymer melt has been proposed: When the fusion

Table 5 The effect of unmelted materials on the subsequent non-isothermal crystallization

Sample	Φ [°C min^{-1}]	T_p [°C]	n	k [s^{-n}]	$\Delta E^{[a]}$ [kJ mol^{-1}]	$\Delta E^{[b]}$ [kJ mol^{-1}]
no or less unmelted materials in the melt	5–20	130.5–125.1	2.0–2.2	1.36×10^{-5}–2.48×10^{-4}	347	352
a lot of unmelted[c] materials in the melt	5–20	138.8–133.0	2.1–2.3	0.04–1.07	266	261

[a] Determined by the Avrami equation
[b] Determined by the Kissinger equation
[c] Cf. ref. [30]

temperature is lower than 170.5 °C, the iPP melt is of a helically ordered structure, so the crystallization proceeds by heterogeneous nucleation with two-dimensional diffusion controlled growth and the Avrami exponent is 2. If the temperature is higher than 170.5 °C, the helically ordered structure of melt is destroyed and the order of the polymer melt is decreased greatly. Consequently, the crystal growth is three-dimensional and the Avrami exponent becomes larger. Furthermore, if some unmelted crystals exist in the helically ordered melt, then the subsequent crystallization would become more rapid.

Acknowledgements This work was subsidized by the Special Funds for Major State Basic Research Projects of China (G1999064800).

References

1. Marker L, Hay PM, Tilley GP, Early RM, Sweeting OJ (1959) J Polym Sci 38:33
2. Griffith JH, Ranby BG (1959) J Polym Sci 38:107
3. Falkai VB, Stuart HA (1959) Kolloid Z 162:138
4. Magill JH (1962) Polymer 3:35
5. Parrini P, Corrieri G (1963) Makromol Chem 62:83
6. Chiu J (1964) Anal Chem 36:2058
7. Gordon M, Hillier IH (1965) Polymer 6:213
8. Hoshino S, Meinecke E, Powers J, Stein RS (1965) J Polym Sci Part A 3:3041
9. Godovsky YK, Slonimsky GL (1974) J Polym Sci Polym Phys Ed 12:1053
10. Pratt CF, Hobbs SY (1976) Polymer 17:12
11. Leute U, Dollhopf W, Liska E (1976) Colloid Polym Sci 254:237
12. Ishizuka O, Koyama K (1977) Polymer 18:913
13. Wlochowicz A, Eder M (1981) Polymer 22:1285
14. Rybnikar F (1982) J Appl Polym Sci 27:1479
15. Martuscelli E, Pracella M, Crispino L (1983) Polymer 24:693
16. Avella M, Martuscelli E, Pracella M (1983) J Therm Anal 28:237
17. Martuscelli E, Pracella M, Volpe GD, Greco P (1984) Makromol Chem 185:1041
18. Carfagna C, Rosa CD, Guerra G, Petraccone V (1984) Polymer 25:1462
19. Kowalewski T, Galeski A (1986) J Appl Polym Sci 32:2919
20. Monasse B, Haudin JM (1986) Colloid Polym Sci 264:117
21. Avella M, Martuscelli E, Sellitti C, Garagnani E (1987) J Mater Sci 22:3185
22. Khanna YP (1990) Polym Eng Sci 30:1615
23. Tai HJ, Chiu WY, Chen LW, Chu LH (1991) J Appl Polym Sci 42:3111
24. Kim YC, Kim CY, Kim SC (1991) Polym Eng Sci 31:1009
25. Piccarolo S, Saiu M, Brucato V, Titomanlio G (1992) J Appl Polym Sci 46:625
26. Kim CY, Kim YC, Kim SC (1993) Polym Eng Sci 33:1445
27. Hieber CA (1995) Polymer 36:1455
28. Alfonso GC, Ziabicki A (1995) Colloid Polym Sci 273:317
29. Bogoeva-Gaceva G, Janevski A, Grozdanov A (1998) J Appl Polym Sci 67:395
30. Zhu XY, Li YJ, Yan DY, Fang YP Polymer accepted
31. Zhu XY, Yan DY, Yao HX, Zhu PF (2000) Macromol Rapid Commun 21:354
32. Zhu XY, Yan DY, Tan SS, Wang T, Yan DH, Zhou E (2000) J Appl Polym Sci 77:163
33. Zhu XY, Yan DY Macromol Chem Phys accepted
34. Zhu XY, Li YJ, Yan DY, Zhu PF, Lu QH (2001) Colloid Polym Sci accepted
35. Avrami M (1939) J Chem Phys 7:1103
36. Avrami M (1940) J Chem Phys 8:212
37. Cebe P, Hong SD (1986) Polymer 27:1183
38. Kissinger HE (1956) J Res Natl Stds 57:217
39. Bank W, Gordon M, Sharples A (1963) Polymer 4:289
40. Tan SS, Su A, Li W, Zhou E (1998) Macromol Rapid Commun 19:11
41. Tan SS, Su A, Luo J, Zhou E (1999) Polymer 40:1223
42. Li YJ, Zhu XY, Yan DY to be published